Summary of the main scientific results obtained in the project

Background

As reported earlier, our industrial partner, who played a fundamental role in the design, construction and servicing of the *Solar Cell Technology Innovation Centre* installed at MFA was BudaSolar Ltd.. Unfortunately, in 2011 the company went bankrupt. Thereby we lost our technical backup, in the existing apparatus the original co-evaporation concept for all four constituents became in this way obsolete. During the one year suspension of the project permitted by the OTKA Collegium we made efforts to find alternative solutions for the hardware deficiency-related issues.

The available linear sources could only be applied for the evaporation of the low melting point metallic components (In, Ga), while the evaporation of Cu, although attempted, did not lead to any usable result without the appropriate source developed and installed. **Therefore, unfortunately we had to divert from the original Workplan.** Also the FTE effort devoted to the project had to be modified. On one hand the final target of characterisation of PV devices containing the co-evaporated quaternary compound absorbers could not be achieved, so the FTE of the researchers responsible for device characterisation dropped-out. On the other hand a lot more effort was put in the hardware-setup and structural-compositional analysis, which not always delivered publishable results. **The factual FTE in the project is17.3**.

In the first place we focussed on the research *objectives related to the layer studies involving ALD*. A systematic study of the Al-doping of ALD ZnO by alternative precursor pulse method was performed [5,7, 27, 28, 29, 30]. The results were applied and published also as substrate for epitaxial growth of ZnO nanorods [10], as well as n-doped electrode in porous Si based polymer-composite solar cells [32].

Secondarily, we had to find *solutions for the replacement of the original co-evaporated CIGS concept by alternative methods*. Besides the evaporation of the metallic components in the main facility we resorted for the fabrication of the quaternary structure to sputtered Cu from the target installed in the sputter unit and post-selenisation by two alternative techniques. In order to keep the conveyor-track clean and further usable for pure metallic precursor deposition, first we installed a separate high vacuum evaporation system for Se. Secondly, we studied the post-selenization under constant vapour pressure [8, 9, 31]. In the final year of the project the main emphasis was placed on the structural-compositional analysis of these CIGS layers [8, 9, 31].

Despite the technical difficulties, all in all the project is considered scientifically and from the educational point of view a success.

- Two PhD thesises were prepared by participants of this OTKA project using the obtained results. Ágoston Németh got his degree [11] from the Budapest University of Technology and Economy in 2010. Zsófia Baji is about to complete her dissertation [12] to be submitted also to the BUTE Doctoral School of Physics in 2012.

- All in all 10 journal papers (three of them being under evaluation) and 20 conference contributions (posters and lectures) were produced with the support of this grant. The conference publications and submitted manuscripts, as well as the complete scientific report are available at: http://www.mfa.kfki.hu/hu/CIGS-OTKA .

– The project contributed to the success of other projects as well, and enhanced the know-how of MFA by introducing the Atomic Layer Deposition being a fundamental tool for nanotechnology.

Being aware of the incomplete realisation of the original Workprogram and FTE reduction, we saved 10% of the original grant, and refund if requested, subject to the decision of the OTKA Collegium.

Introduction

Referring to the project proposal, "this project is a concerted, complex experimental approach of research groups in different research institutions to *elucidate upon the fundamental physical and chemical phenomena guiding the growth of multi-component semiconductor thin films* on large flat metalized glass substrates. Admittedly, *this is a „targeted research"- type fundamental research attempt rather than being a curiosity-driven type research."* The sample preparation experiments were meant to be performed in the *Solar Cell Innovation Center of MFA developed as an R&D facility for thin film solar cells with CuInGaSe active layer.* The cross-section of the solar cell structure is shown in Fig. 1.

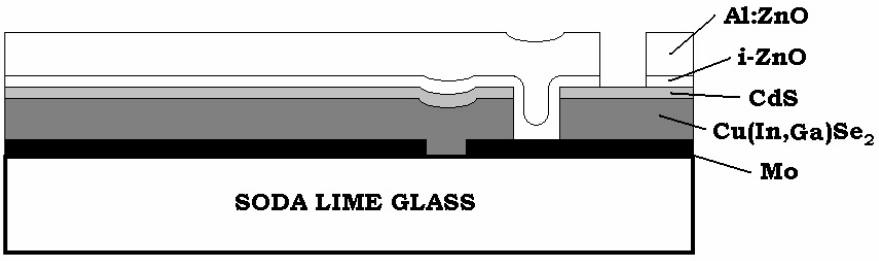

"The *subject of the present materials research project is the active region of the structure*, the p-type CIGS layer (grey) and the n-type buffer layer (here CdS) on top of it. The corresponding band diagram is shown below.

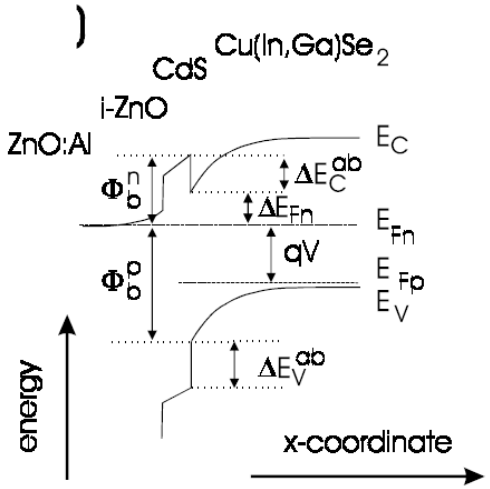

Fig. 1. a The different layers of a ZnO/CdS/CuIn(Ga)Se_2 heterojunction solar cell. **b** Band diagram of the heterojunction with the conduction and valence band energies E_C and E_V, an applied bias voltage V. The quantities Φ_b^p and Φ_b^n denote the barriers for holes and electrons as described in the text, ΔE_{Fn} is the energy distance between the Fermi level and the conduction band energy at the CdS/CuIn(Ga)Se_2 heterointerface, ΔE_V^{ab} and ΔE_C^{ab} are the valence band and conduction band discontinuities at the buffer absorber interface

The experimental vacuum-facility (*Solar Cell Innovation Center),* however, only contained the sputtering, the evaporation(partly) and annealing, as well as the laser patterning capabilities. Therefore, the n-type buffer-layer, mostly CdS had to be added as a wet chemical step to the otherwise fully automated fabrication scheme, interrupting the closed-loop cycle in the vacuum apparatus equipped with a conveyor-type transport system. In order to avoid this,

one of the main targets of this project was to find a vacuum-compatible alternative for the buffer-layer growth, which in the perspective can be integrated into the exisiting manufacturing line.

Introduction of the ALD technique

The option selected was the **Atomic Layer Deposition,** a vacuum-deposition technique allowing monolayer growth control. The fundamental research aimed at **the study of the conformal deposition of thin, controlled n-doped ZnO semiconducting layers** *intended to replace the CdS buffers* [24, 25]. This technique, however, was not available in Hungary at the beginning. We initiated a collaboration with a Finnish company, Picosun Oy to develop the system of our choice for off-line experiments. The SUNALE™ ALD reactor with a pneumatic lift was purchased and installed using the grant of OTKA in this grant NK73424. The Atomic Layer Deposition (ALD) facility used throughout the project was installed in the cleanroom of the Microtechnology Department of MFA.

Main technical characteristics of the ALD equipment are: - Substrate size: 4’ wafer - No. of sources: four in total, including a Picosolid™ booster source -Tested for Al_2O_3 and ZnO	

In the project ALD grown ZnO layers were systematically studied, how the incorporation of different Al contents determines the semiconducting properties of the layers. We developed an ALD process for the in situ Al doping of ZnO, the *novel alternate precursor pulse method [5, 7, 27, 28, 29]*. The procedure consists of periodic alternate injection of Al-precursor pulses intermixed with the sequences of Zn-precursor pulses. In this way Al is incorporated as constituent of the growing layer, although it is uncertain, how: what fraction of it occupies substitutional sites in the growing ZnO matrix, and acts as dopant in the semiconducting oxide.

The specific resistance of the ALD Al:ZnO layers were evaluated as a function of the introduced atomic fraction of Al (i.e. number of Al precursor pulses) and temperature. It was found that both the temperature- and doping dependence of the resistivity develop a minimum: the optimal doping of the ALD deposited Al-ZnO is obtained around 2 at% at 210-240°C substrate temperature, as shown in the coloured 3D plot [5]. The figure summarizes the specific resistivity of the layers as a function of the Al content and substrate temperature. We found that the aluminium incorporation up to a certain amount of Al content decreases the resistivity of zinc-oxide layers, and above that threshold value the resistivity starts to increase again.

We characterised systematically the obtained carrier concentration and carrier mobility by Hall measurements vs.ALD growth temperature and atomic % of Al incorporated, in order to determine the active dopant contribution [7].

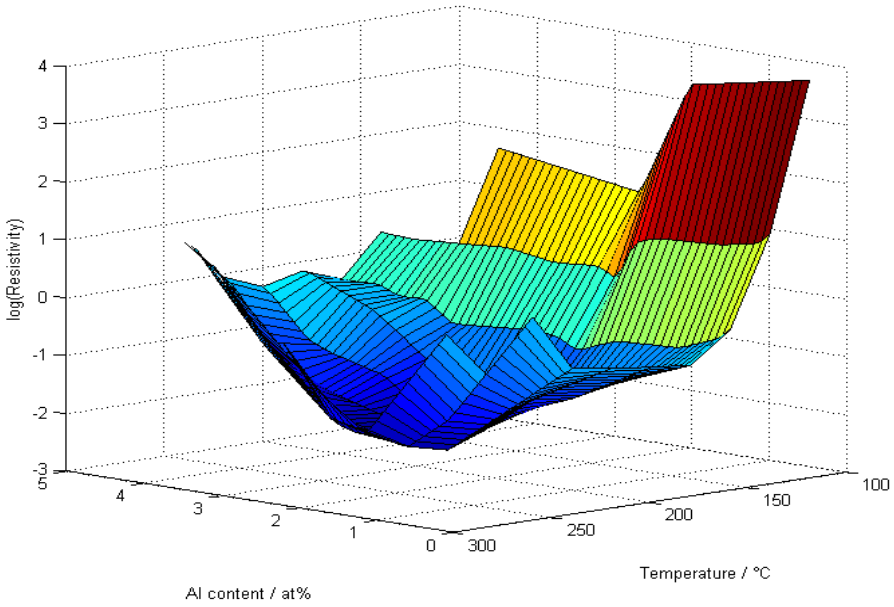
log(Resistivity)
4
3
2
1
0
-1
-2
-3
5
4
3
2
1
0
Al content / at%
300
250
200
150
100
Temperature / °C

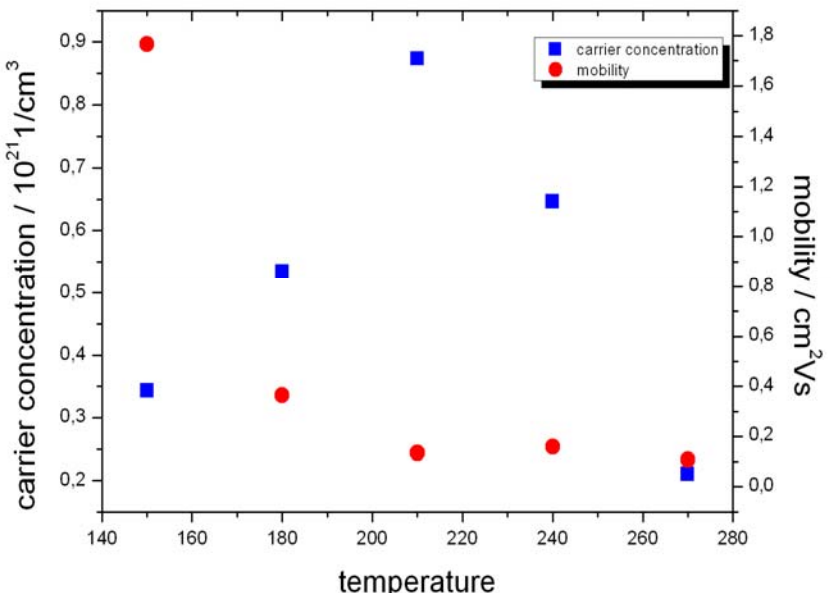
carrier concentration
mobility
carrier concentration / 10^{21}1/cm^3
mobility / cm^2/Vs
0,9
0,8
0,7
0,6
0,5
0,4
0,3
0,2
1,8
1,6
1,4
1,2
1,0
0,8
0,6
0,4
0,2
0,0
140
160
180
200
220
240
260
280
temperature

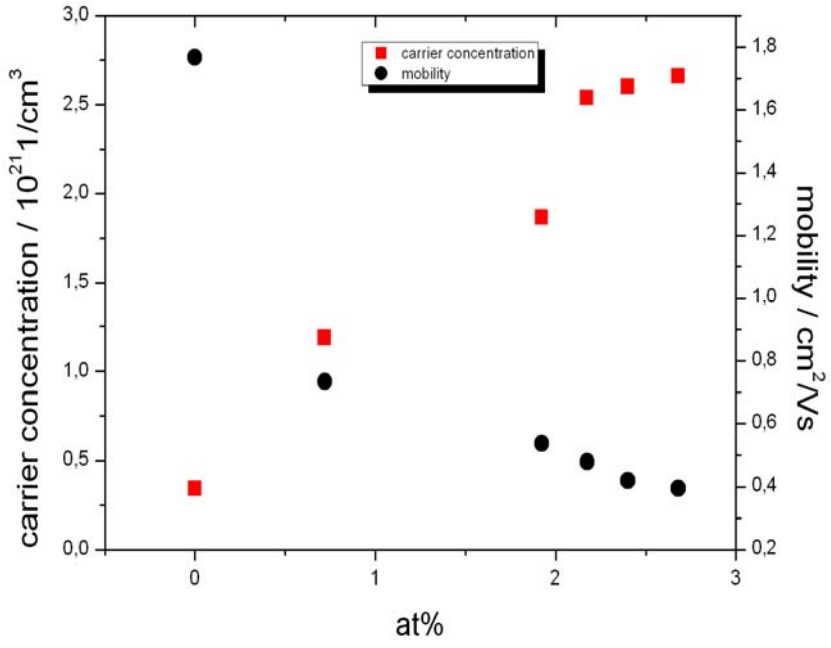
carrier concentration
mobility
carrier concentration / 10^{21}1/cm^3
mobility / cm^2/Vs
3,0
2,5
2,0
1,5
1,0
0,5
0,0
1,8
1,6
1,4
1,2
1,0
0,8
0,6
0,4
0,2
0
1
2
3
at%

Spectroscopic ellipsometry results on the Al-doped ALD layers revealed that the *majority of aluminium is present in form of Al_2O_3 [32].* However, not in a separate phase (as verified by XRD). The layers are rather homogenous mixtures of ZnO and Al_2O_3. *The electrically active fraction of the Al content is sufficient to reduce the resistivity of the layers by two orders of magnitude.* The aluminium incorporation reduces the grain size in the layers.

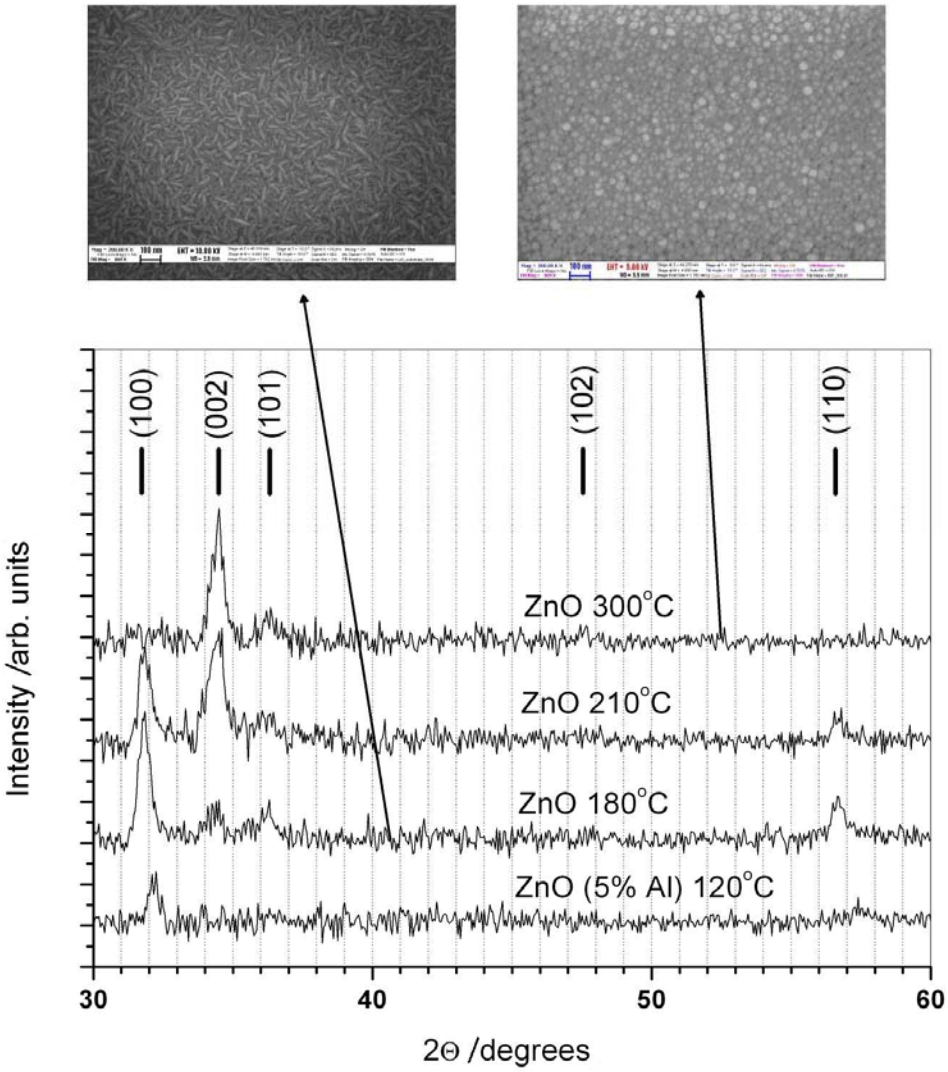

A relationship between crystalline morphology vs. temperature and aluminium incorporation was established. The above figure summarizes the XRD characterization results of our samples. Two characteristic SEM micrographs are also presented, reflecting the morphology for the two preferential crystalline orientations in the ZnO layers. These are the (100), when the c axis of the ZnO unit cell is parallel with the substrate, and the (002), where the c axis is normal to the surface [7].

The preferred crystalline orientation of the layers depends on the deposition temperature and the aluminium concentration as well. The crystalline quality, orientation and the grain size are all determined by these parameters. X-ray diffraction analysis revealed a change in the dominant crystallite orientation with increasing substrate temperature. *The most perfect crystal structure and largest grain size was found with 2at% aluminium.* In ca. 200 cycles of alternating Zn and ca. 2at% Al precursor pulses Al-doped ZnO layers on glass substrates could be formed reliably at T= 210-220°C with n=1,2•1021cm-3 doping concentration, μ= 0.7 cm2/Vs mobility and ρ≈2 mΩcm (1 vs. 7 mΩcm lateral and normal) resistivity.

Accumulation of compressive strain developed a monotonous increase with the growth temperature. Electric resistivity showed no significant anisotropy despite of the change in the orientation the dominant conduction mechanism is not grain boundary related [7, 27].

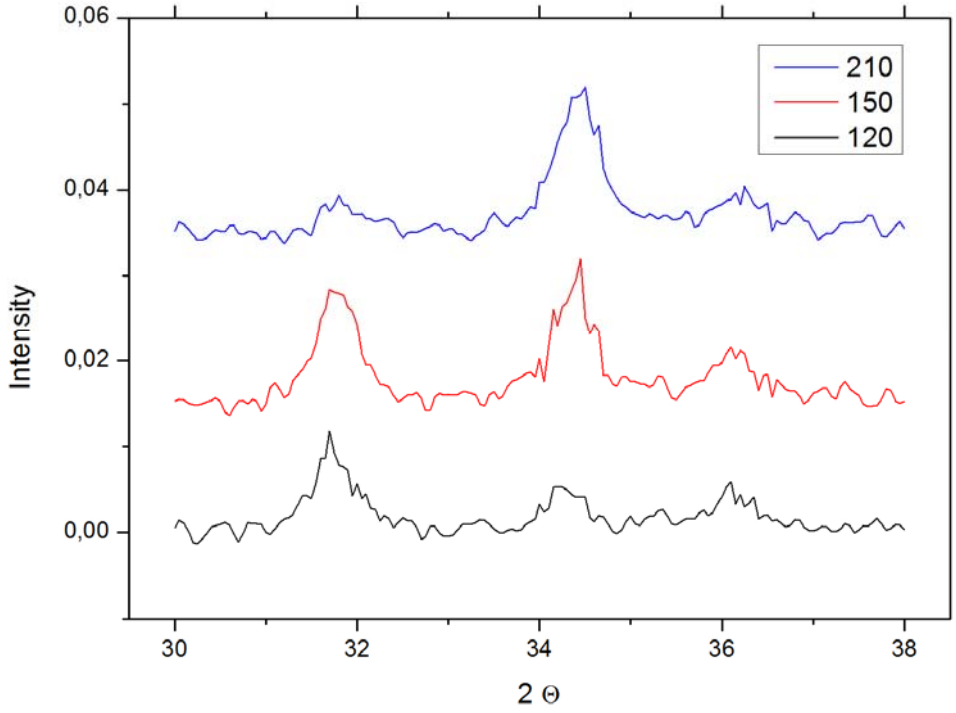

The intrinsic ZnO samples above were deposited at three different substrate temperatures (120°C, 150°C, 210°C) and their spectra can be considered typical The most intensive XRD peaks can be found at *2Θ= 31,77° the (100), at 2Θ= 34,42° the (002), and at 2Θ=36,25° the (101), respectively [5]*. We could state that:

- (100) and (002) orientations are the most prominent;

- in most samples a low (101) peak is also present, but never well pronounced;

- increasing deposition temperature causes a shift of the intensities, i.e. (100) peak decays with the increasing temperature while peak (002) becomes more prominent. This phenomenon is in agreement with the literature results.

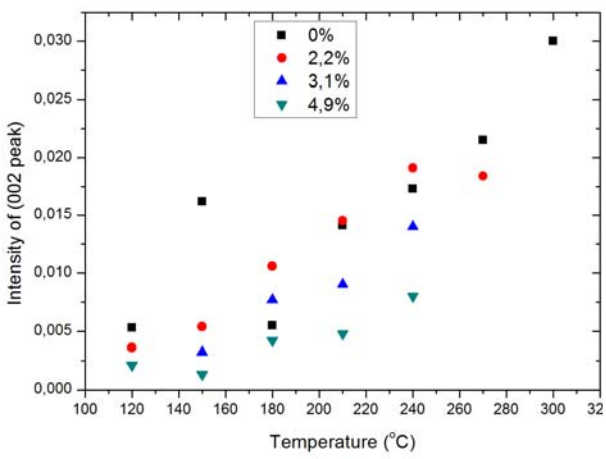

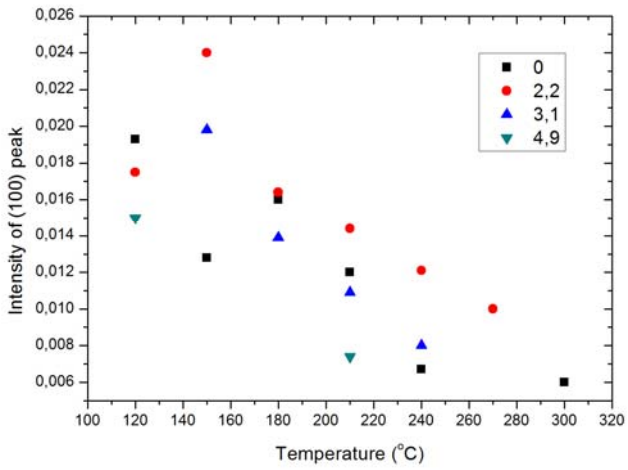

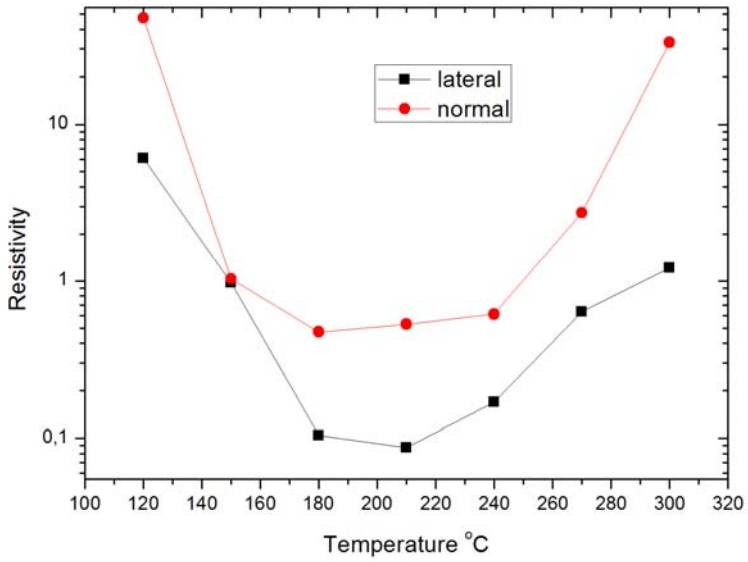

Specific resistance (in $X10^{-2}$ cm^{-3}) of the 2 at% Al-doped sample parallel and perpendicular to the layer surface vs. deposition temperature for the determination of the optimum growth conditions [7, 27].

The developed vacuum-process for the in situ Al doping of ZnO consisting of periodic alternating injection of Al-precursor pulses intermixed with the sequences of Zn-precursor pulses in ALD without post-annealing is stable and reproducible.

Growth conditions	**ALD parameters**
Precursors:	Diethyl zinc and Trimethyl aluminium
Oxidant:	H_2O
Process pressure:	10-15 hPa
Substrates:	GaN
Deposition temperature:	210-300°C
Cycle sequence:	$(i(DEZn+H_2O)+TMAl+H_2O)j+i(DEZn+H_2O)$, with $9<i<60$
Reservoire temperature:	24°C
Injection time:	0,1 s
Purge time:	3 s
Flow rates:	Precursors:150sccm, H_2O: 300 sccm

X-ray diffraction analysis revealed a *change in the dominant crystallite orientation in the layers with increasing deposition temperature*. ***The most perfect crystal structure and largest grain size was obtained with 2at% Al at every growth temperature***, while the accumulation of compressive strain developed a monotonous increase with the growth temperature.

Electrical resistivity revealed no anisotropy despite of the obvious change in the orientation, i.e. the conduction mechanism is not dominated by grain boundary effects [7].

ALD being a layer-by-layer deposition method, we studied - beyond the direct workprogram of this project, as part of the PhD research of Zs. Baji - the *growth of epitaxial ZnO layers*, too [33]. ZnO epitaxy can be grown on GaN at temperatures above 270°. It was

determined that

- The conductivity of the epitaxial layers falls between 1 and 2·10 -4 Ωcm.
- Already 12 pulses of Al_2O_3 deteriorate the epitaxy, although these are still high quality oriented layers.
- The doping only reduces the resistivity by 30%.

The growth of single-crystalline Zn-nanowires on reactively sputtered, doped polycrytalline ZnO substrates developed int he PhD thesis of Á. Németh was studied earlier [1, 11,13]. Now we tried to use the epitaxial ALD layers [33] as substrates for the oredered growth of ZnO nanorods with success. The results are about to be published:

> Z. Szabo, J. Volk, Zs. Baji, Z. Labadi, I. Barsony, „Epitaxial ALD ZnO templates for highly ordered nanorods" to be submitted to J. Crystal Growth

CIGS absorber layer research

The other main target in the original workprogram of this OTKA research was **to elucidate upon the controlled preparation and properties of coevaporated ternary compound CIGS absorber layers.** We made all efforts, as reported in the first two years of the project, to accelerate the development of the required line-sources for the evaporation cluster of the closed-loop vacuum processing equipment with our industrial partner BudaSolar Ltd. As we duly reported, this attempt was prone to fail, which forced us to apply for a one year suspension of the spending from the project's budget, and try to find alternative solutions to complete the research.

A novel fabrication method for $Cu(InGa)Se_2$ was developed by using flash-like evaporation of metallic precursors followed by post-selenization [8, 28, 31]. Unlike the processes using consecutive evaporation or simultaneous co-evaporation of precursors from multiple sources, this flash method evaporates the metallic components from a single boat at the same time. The main advantage of this method is its simplicity.

Post-selenization was carried out in sealed ampoules under constant Se vapour-pressure. The resulting layers are homogenous CIGS films with the required composition and crystalline structure.

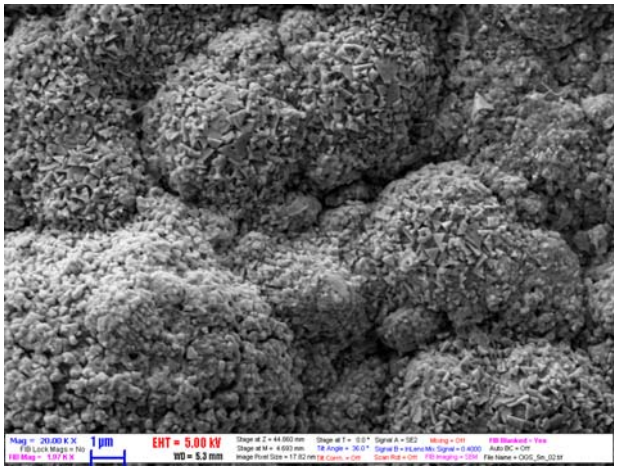

SEM micrograph of the flash evaporated and post selenized (500°C for 15 min) CIGS layer. Note the cauliflower-like morphology [8].

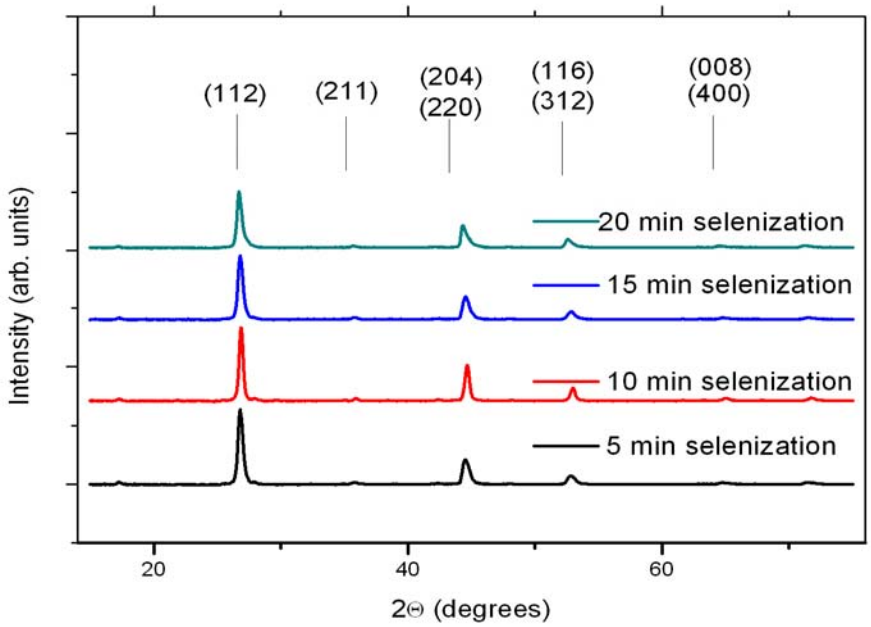

XPS results obtained on the CIGS layers post-selenized at 500°C for different durations. Only the diffraction peaks of the chalcopyrite structure are present, no oxides or selenides are visible, whatsoever [8].

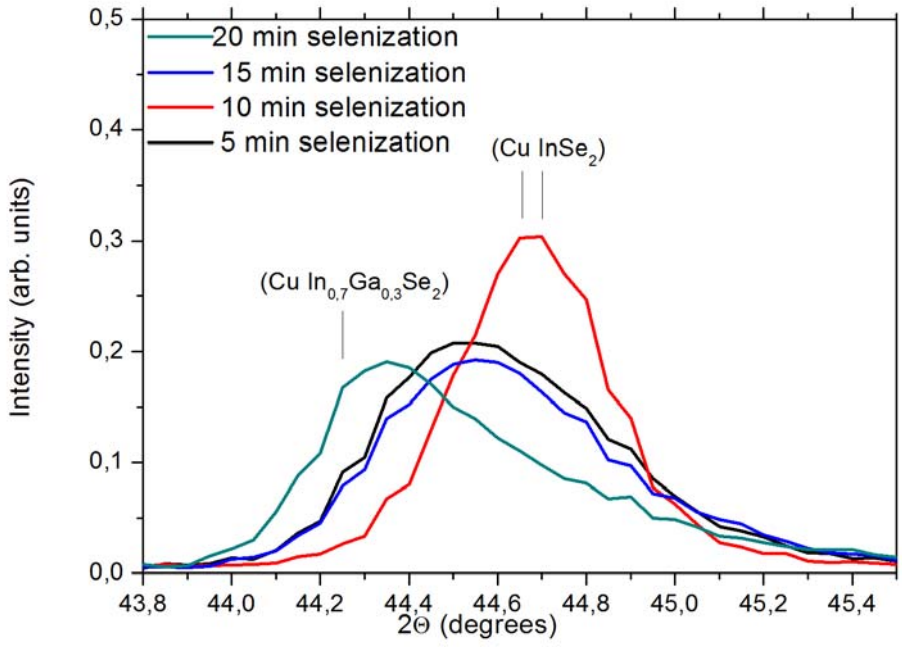

Selenization time only affected the Ga content according to the zoomed-in intensity plot [8].

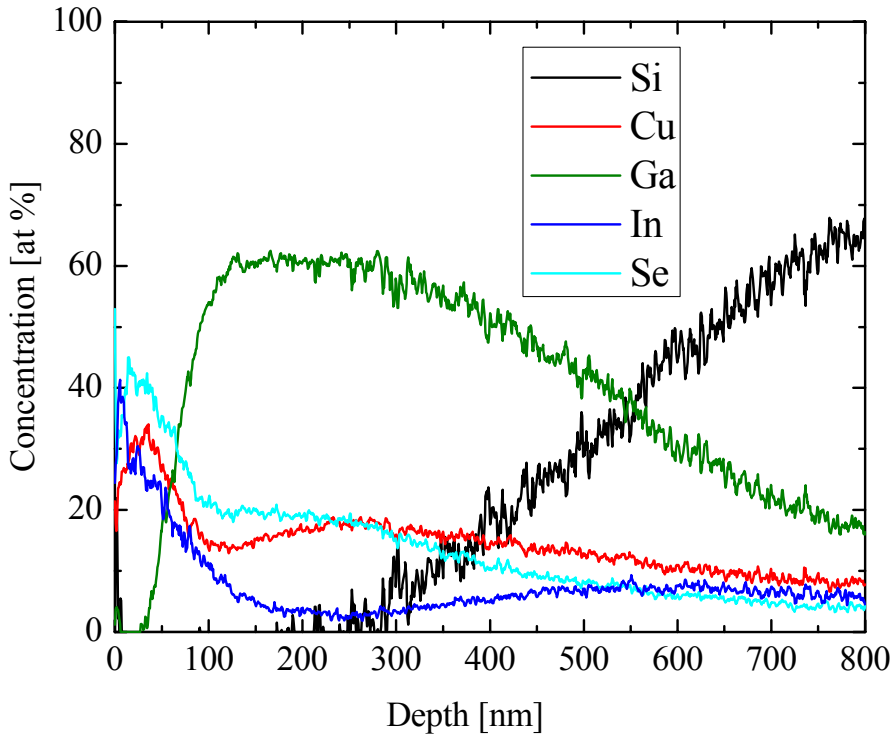

SNMS depth profiles of the CIGS layer selenized at 500° for 15 minutes. In this concentration plot no Ga accumulation was observable at the bottom of the CIGS layer, the depth of which is indicated by the increase of the Si concentration originating from the glass substrate [8].

In conclusion contrary to the report by Su et al. we found no negative effect of the rough precursor morphology on the morphology and structure of the final CIGS layers. The post selenization not only forms the absorber layer but also smoothens the CIG precursor morphology.

$CuIn_{0,8}Ga_{0,2}Se_2$ composition considered ideal for photovoltaic application was found in samples selenized for 10 to 15 min. SNMS spectra of the film proved the uniform Ga concentration across the whole thickness [31].

In a parallel study the **possibility of fabrication of CIGS layers from stacked precursors with post-selenization** has been examined. Different sequences of precursor layers and two different selenization methods were applied, in order to establish the *optimal order of Cu, In and Ga layers in the precursor layer-stack*.

An extensive use of SEM, both cross section and top view as well as element analysis of a large number of samples obtained from the experiments facilitated the selection of the best candidates for the detailed XRD analysis and SNMS profiling. Again the uneven surface of the structures introduced uncertainties in the time-depth scale conversion, but in most of the cases reliable qualitative and even semi-quantitative conclusions could be drawn.

The following table summarizes the systematic experiments with the sample numbers indicated.

1	Mo	In	Ga	Cu	Selenization with Se evaporation and annealing
2	Mo	Ga	In	Cu	Selenization with Se evaporation and annealing
3	Mo	Cu	In	Ga	Selenization with Se evaporation and annealing
4	Mo	Cu	Ga	In	Selenization with Se evaporation and annealing
5	Mo	In	Ga	Cu	Selenization with Se vapour
6	Mo	Ga	In	Cu	Selenization with Se vapour
7	Mo	Cu	In	Ga	Selenization with Se vapour
8	Mo	Cu	Ga	In	Selenization with Se vapour

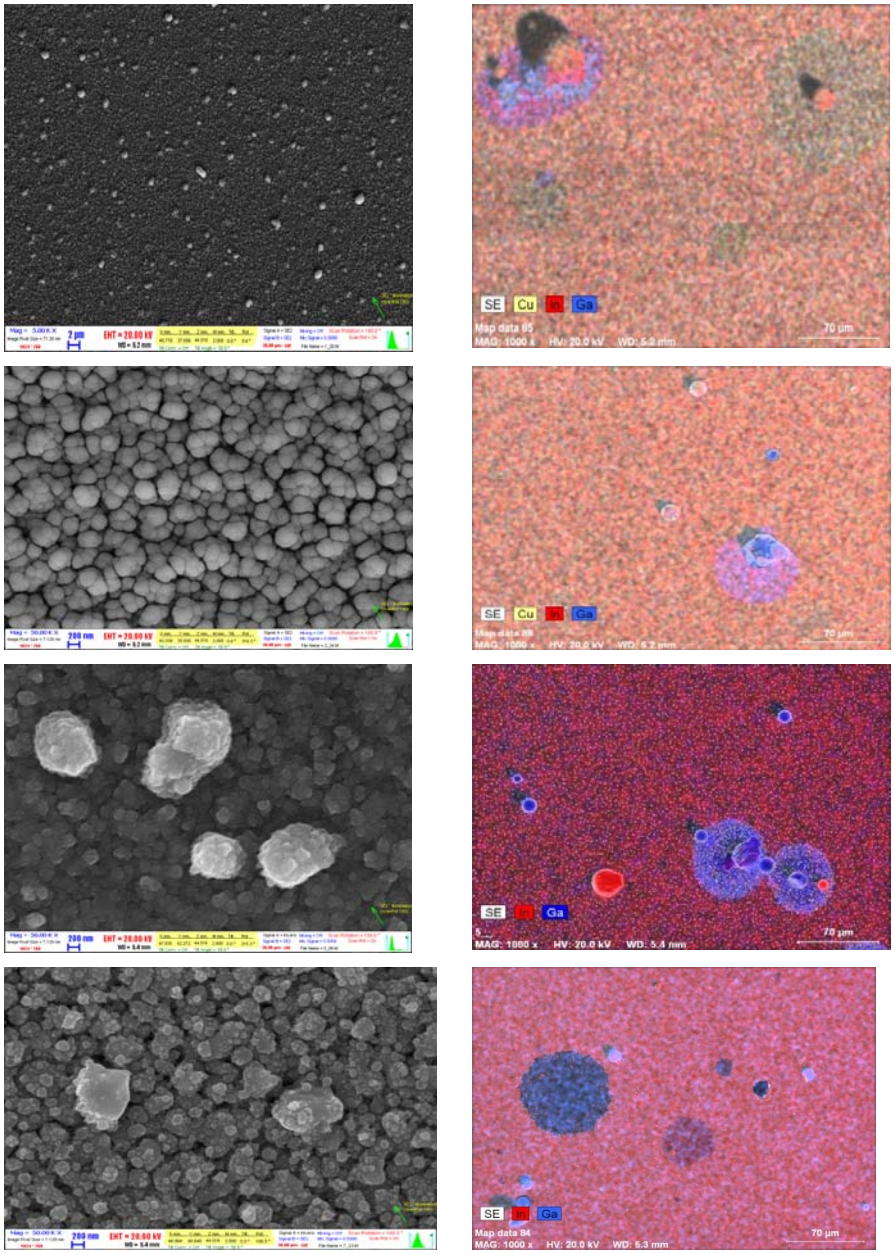

SEM micrographs (left) at 5000x in (a) and 50000x magnification (c,e,g) and element maps of the evaporated precursors (right) for sample 1, 2, 3 and 4 in the respective rows [9].

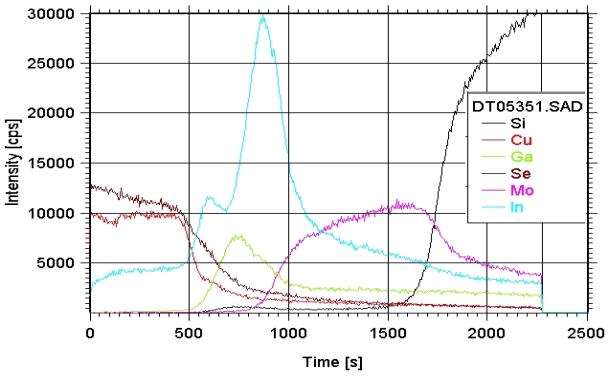
DT05351.SAD
Si
Cu
Ga
Se
Mo
In
Intensity [cps]
Time [s]

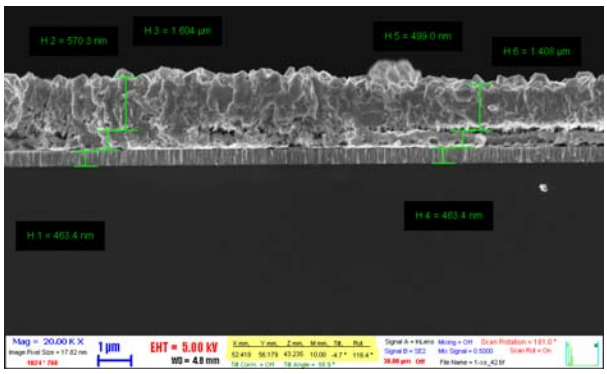
H 2 = 570.3 nm
H 3 = 1.604 µm
H 5 = 499.0 nm
H 6 = 1.408 µm
H 4 = 463.4 nm
H 1 = 463.4 nm
Mag = 20.00 K X
1 µm
EHT = 5.00 kV
WD = 4.8 mm

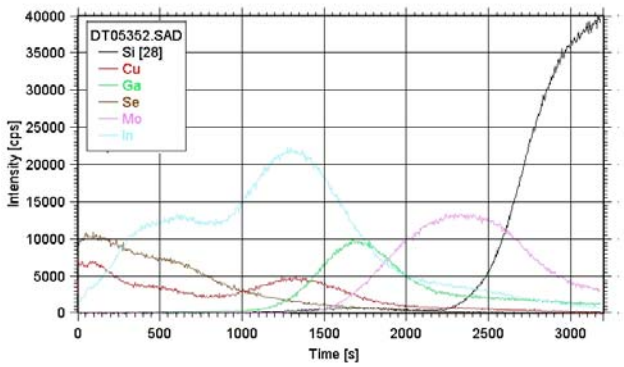
DT05352.SAD
Si [28]
Cu
Ga
Se
Mo
In
Intensity [cps]
Time [s]

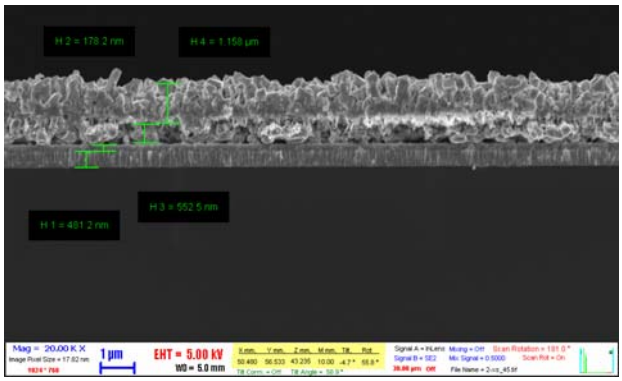
H 2 = 178.2 nm
H 4 = 1.158 µm
H 3 = 552.5 nm
H 1 = 481.2 nm
Mag = 20.00 K X
1 µm
EHT = 5.00 kV
WD = 5.0 mm

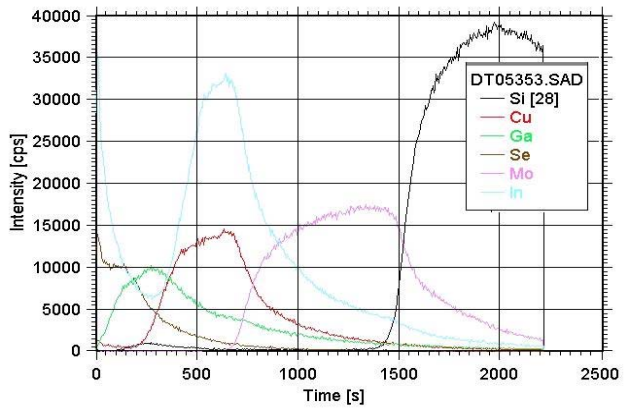
DT05353.SAD
Si [28]
Cu
Ga
Se
Mo
In
Intensity [cps]
Time [s]

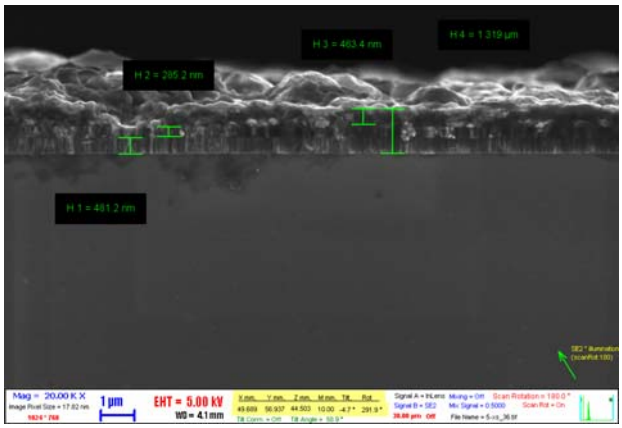
H 3 = 463.4 nm
H 4 = 1.319 µm
H 2 = 285.2 nm
H 1 = 481.2 nm
Mag = 20.00 K X
1 µm
EHT = 5.00 kV
WD = 4.1 mm

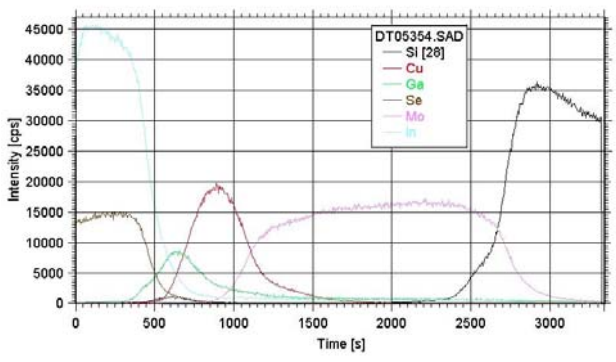
DT05354.SAD
Si [28]
Cu
Ga
Se
Mo
In
Intensity [cps]
Time [s]

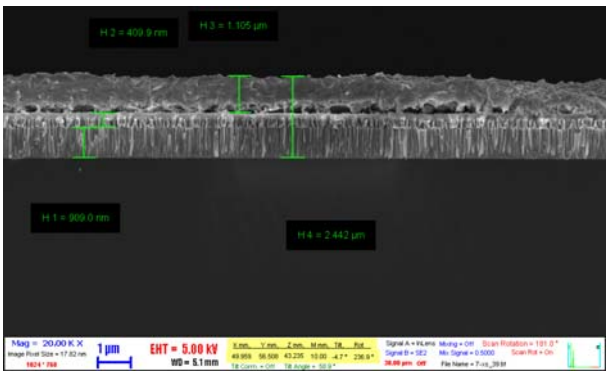
H 2 = 409.9 nm
H 3 = 1.105 µm
H 1 = 909.0 nm
H 4 = 2.442 µm
Mag = 20.00 K X
1 µm
EHT = 5.00 kV
WD = 5.1 mm

In the above figure the SNMS depth profiles (left) and the corresponding SEM cross sections (right) are shown for the *samples selenized with Se evaporation*: Samples 1, 2, 3 and 4 in the respective rows [9]. Interpretation has to take into account the rough morphology-related uncertainties! Comparing these results with the cross sectional SEM images in the right column the thickness of the selenized CIGS layers and that of the unreacted precursor film, which remained underneath, may be defined.

The layers of the precursor metals are still visible, in the original order of the deposition since *the metals did not mix with each other and the alloy formation was negligible at the temperature of the selenization*. On the other hand, as the Se diffused into the layer, a mixing of the components started, which can be concluded from the way the In layer always diffuses towards the surface. The In concentration rapidly increases in the Se-containing top layer. Therefore, the *local minima in the In depth profile indicate chemical reactions*.

The XRD spectra revealed that all the layers contained chalcopyrite phase, some also had one of the metallic precursors in excess. A summary of the crystalline quality of the layers is given in the table below.

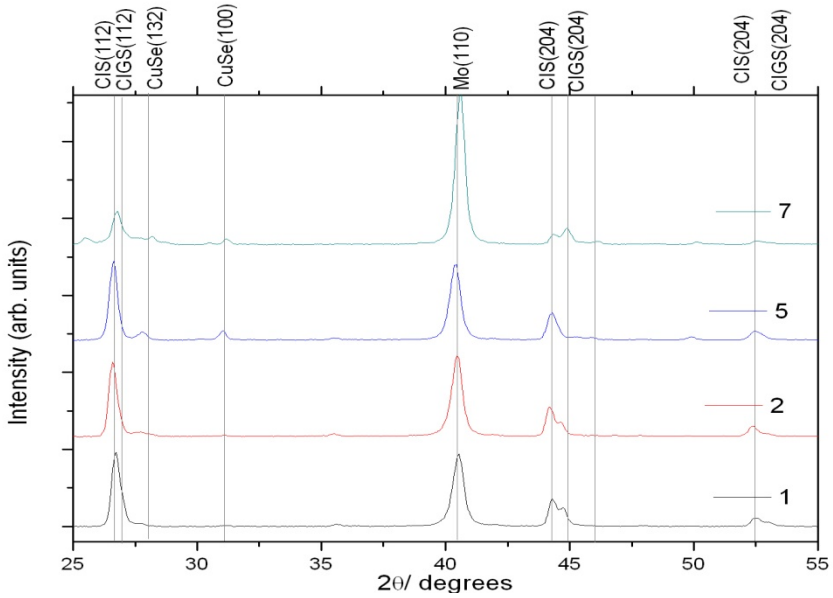

Comparison of the XRD spectra of differently processed CIGS layers (samples 1, 2, 5 and 7).
Summary of the phases identified by XRD in the samples 5-8. selenized with constant vapour pressure.

5	Predominantly $CuIn_{0,7}Ga_{0.3}Se_2$ with a little $CuInSe_2$ phase present.
6	Both $CuInSe_2$ and $CuIn_{0,7}Ga_{0.3}Se_2$ phases present, the $CuInSe_2$ phase is more dominant.
7	Only one chalcopyrite phase present, that of $CuIn_{0,9}Ga_{0.1}Se_2$ with some hexagonal CuSe.
8	$CuInSe_2$ and $CuIn_{0,7}Ga_{0.3}Se_2$ phases with a little hexagonal CuSe present.

SNMS depth profiles (left) and corresponding SEM cross sections (right) of the samples 5, 6, 7 and 8 selenized in constant Se vapour in the rows 1-4, respectively. Interpretation has to take into account the rough morphology-related uncertainties!

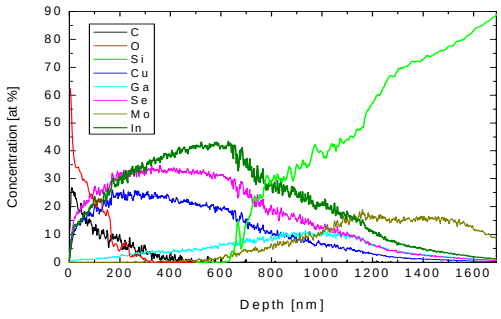
C
O
Si
Cu
Ga
Se
Mo
In
Concentration [at %]
Depth [nm]

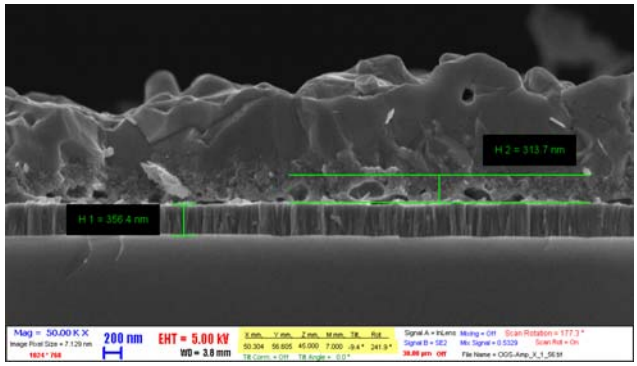
H 2 = 313.7 nm
H 1 = 356.4 nm
200 nm
EHT = 5.00 kV
WD = 3.6 mm

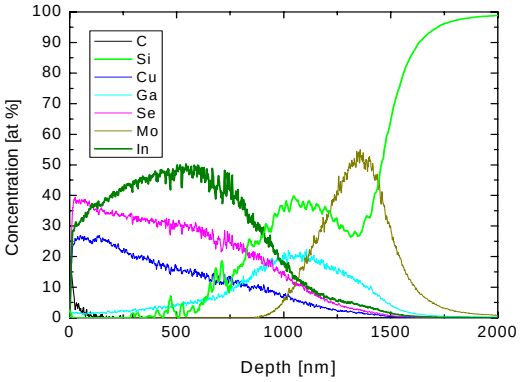
C
Si
Cu
Ga
Se
Mo
In
Concentration [at %]
Depth [nm]

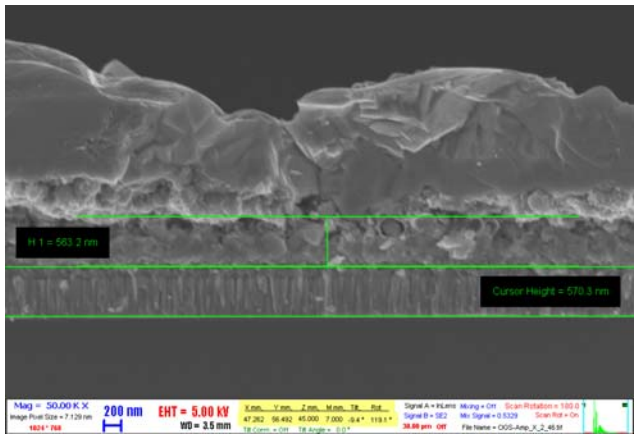
H 1 = 583.2 nm
Cursor Height = 570.3 nm
200 nm
EHT = 5.00 kV
WD = 3.5 mm

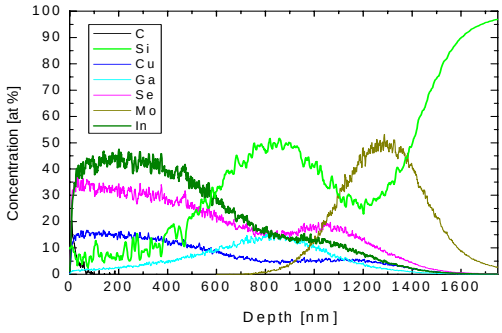
C
Si
Cu
Ga
Se
Mo
In
Concentration [at %]
Depth [nm]

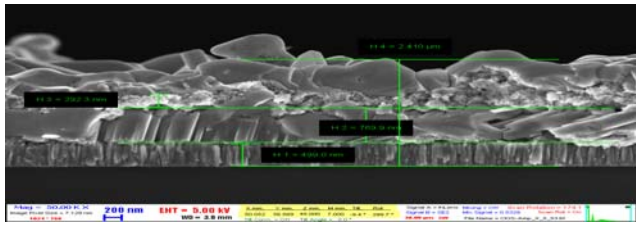

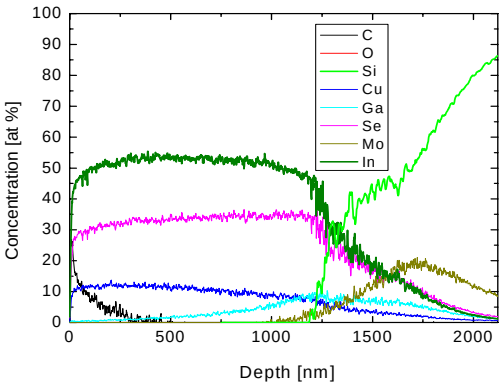
C
O
Si
Cu
Ga
Se
Mo
In
Concentration [at %]
Depth [nm]

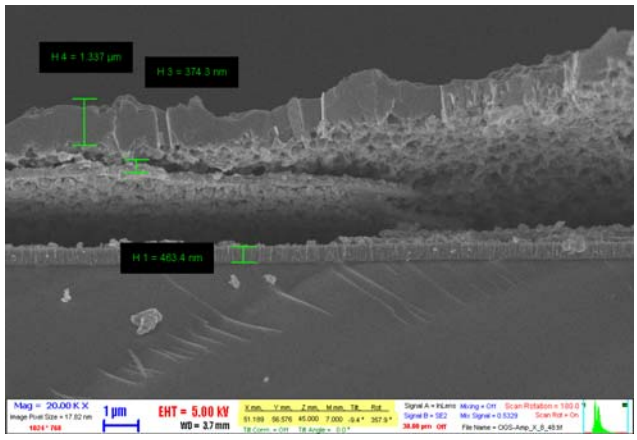
H 4 = 1.337 µm
H 3 = 374.3 nm
H 1 = 463.4 nm
1 µm
EHT = 5.00 kV
WD = 3.7 mm

The absence of binary phases and the $CuInGaSe_2$ phase in case of the samples 5 and 6 indicates that the selenization reaction was complete. The two different layers apparent in the cross sectional images may be the CIS and the CIGS phases, therefore a phase separation must have taken place with the CIS at the top and the CIGS dominantly at the bottom of the layer stack. In samples 7 and 8, however, CuSe is still present. The hexagonal phase CuSe forms probably the crystallites occurring in the SEM micrographs in Fig. 3b. Since in these samples the copper was sputtered first, i.e. Cu was the bottom layer in the layer structure, which is probably why some CuSe was left in the samples. Therefore, this layer structure is either less favourable, or it requires a longer annealing time. Sample 8 also reflected a separation of the phases CIGS and CIS. It is obvious from the XRD results that where Ga is lying deeper in the layer stack than In, the phase separation is more pronounced.

In order to confirm the phase-analysis results, an XPS study was carried out. XPS binding energies were evaluated using the NIST XPS binding energy database. The accuracy of our measurement is within ± 0.1 eV.

Specimen	**Se 3d**	**In 4d 5/2**	**Cu 2p 3/2**
Sample 8	54,4 eV	444,5 eV	932,5 eV
Reference CIGS (own measurement)	54,45 eV	444,6 eV	-
Reference [16] $CuInSe_2$	54.3-54.5 eV	444.6…444.8 eV	932.1-932.6 eV
Cu metal (own measurements)			932,35 eV
In metal		443,9 eV	
Se	55,2 eV		

XPS binding energies of Se, In and Cu measured obtained on sample 8 (post-selenized in constant Se vapour) and a *co-evaporated foreign reference sample* (by courtesy of Prof. Rob Collins, University of Toledo, OH) are in good agreement with the XRD data and *confirm the presence of $CuInSe_2$ and $CuIn_{0,7}Ga_{0.3}Se_2$ phases in sample 8.*

In conclusion from the *comparison of both different post-selenization methods* elaborated on the consecutively evaporated components of the quaternary CIGS structure we found that *the evaporation of Se and subsequent annealing is not sufficient for all the reactions needed to result in a homogeneous CIGS layer***.** Therefore, the **proper selenization must be performed by an annealing in Se-vapour.**

Generally, layers with Cu on top provide better CIGS compositions with both selenization methods. The reason for that is probably that both In and Ga diffuse faster in a Cu rich environment [9].

Interestingly with In atop of Ga more CIS is present. On the other hand the CGS phase was never identified in the layers, not even with Ga on top. This is explained by the diffusion of In towards the Se-rich surface, leading to a more homogeneous precursor structure.

We determined the optimum sequence in the deposition of the precursor metals. Cu sputtering as top layer is most favourable for subsequent selenisation, as it ensures to some extent a mixing of the layers. During sputtering of Cu namely Ga-outdiffusion can take place. On the other hand In has to be covered by Ga in the layer stack, therefore **the optimal sequence is: In, Ga, Cu followed by post-selenization in Se vapour**, since the evaporation of a Se layer and post-annealing does not result in a homogeneous CIGS layer.

List of publications in the project

Journal papers

1. Á. Németh, Z. Lábadi, L. Tóth, I. Bársony, Oscillations and power dependent hysteresis in reactive ZnO plasma, Vacuum, Volume 84, Issue 1, (2009), pp.218-220
2. A. Csik, M. Serényi, Z. Erdélyi, A. Nemcsics, C. Cserhati, G.A. Langer, D.L. Beke, C. Frigeri, A. Simon: Investigation of thermal stability of hydrogenated amorphous Si/Ge multilayers, Vacuum Volume 84, Issue 1, (2009), pp.137-140
3. Simon, A. Sulyok, M. Novák, G. Juhász, T. Lohner, M. Fried, A. Barna, R. Huszank, M. Menyhárd: Investigation of an ion-milled Si/Cr multilayer using micro-RBS, ellipsometry and AES depth pro.ling techniques, Nuclear Instruments and Methods in Physics Research B, Volume 267, Issues 12-13, (2009), pp. 2212-2215
4. C. Major, Á. Németh, G.Radnoczi, Z. Czigany, M. Fried, Z. Labadi, I. Barsony: Optical and electrical chracterisation of aluminium doped ZnO layers, Applied Surface Science, Volume 255, Issue 21, (2009) pp. 8907-8912
5. Zs. Baji, Z. Lábadi, Zs. E. Horváth, M. Fried, B. Szentpáli, I. Bársony Temperature dependent in situ doping of ALD ZnO, Journal of Thermal Analysis and Calorimetry, 105 (1) (2011) pp. 93-99
6. Zs. Baji, A. Szanyo, Gy. Molnár, A. L. Tóth, G. Pető, K. Frey,E. Kotai, and G. Kaptay, Formation of Nanoparticles by Ion Beam Irradiation of Thin Films, Journal of Nanoscience and Nanotechnology, Vol. 12, (2012) pp. 1-7.
7. Zs. Baji, Z. Lábadi, Z. E. Horváth, I. Bársony, Structure and morphology of aluminium doped Zinc-oxide layers prepared by atomic layer deposition, Thin Solid Films 520 (2012), pp. 4703-4706
8. Zs. Baji, Z. Lábadi, Gy. Molnár, A. L. Tóth, I. Bársony: CIGS films prepared by flash evaporation and post selenization, Submitted to Thin Solid Films
9. Zs. Baji, Z. Lábadi, Gy. Molnár, A. L. Tóth, K. Vad, I. Bársony: Post-selenization of stacked precursor layers for CIGS Submitted to Materials Science and Engineering B
10. Z. Szabó, J. Volk, E. Fülöp, A. Deák, I. Bársony: Regular ZnO nanopillar arrays by nanosphere photolithography Submitted to Photonics and Nanostructures

PhD Theses

11. Ágoston Nemeth: “ZnO vékonyrétegek vizsgálata”, (Characterization of ZnO thin films) PhD. Thesis, BME VIK, MTA MFA, 2009
12. Baji Zsófia: Semiconductor thin films for solar cell purposes, PhD Thesis, BME Fizikai tudományok doktori iskola, MTA TTK MFA, 2012, to be submitted

Conference proceedings, posters and lectures

13. Á. Németh, Z. Lábadi, B. Gergely, I. Bársony, Oscillation and hysteresis in the reactive plasma during ZnO deposition, 6-th Solid State Surfaces and Interfaces Confernce, November 24 – 27, 2008 Smolenice Castle, Slovakia – oral presentation
14. Á. Németh, Z. Lábadi, L. Tóth, I. Bársony, Oscillations and power dependent hysteresis in reactive ZnO plasma, JVC12-EVC10-AMDVG7 22-26 September 2008, Balatonalmádi, Hungary
15. A. Simon, R. Huszank, M. Novak, Z. Pintye: Investigation of hydrogen depletion of organic materials upon ion-beam irradiation by simultaneous micro-RBS and micro-ERDA technics, 19th International Conference on ion-beam analysis, Cambridge, UK, 7-11, Septembre, 2009
16. A. Buzas, Z. Geretovszky, A. Nemeth, Z. Labadi, G. Juhasz, C. Major, I. Barsony: Selective laser cutting of ZnO:Al contact layers, Proceedings of the 24th European PV Solar Energy Conference, Hamburg GE, 21-25 Septembre, 2009
17. A. Csík, G.A. Langer, L. Péter, K. Vad: Ipari felületi rétegek vizsgálata Szekunder Semleges Részecske Tömegspektrométerrel, ELFT Őszi Iskola, Gyöngyöstarján, Szeptember 30., 2009
18. A. Csík, K. Vad, G.A. Langer: Application of Secondary Neutral Mass Spectrometry for quantitative elemental and depth profile analysis, Ukrainian-Hungarian Workshop, Uzhgorod, Ukraine, November 3,, 2009
19. B.. Szentpali, Á. Németh, Z. Labadi, Gy. Kovacs: The low-frequency noise in Al doped ZnO films, Proceedings of the 20th International Conference on Noise and Fluctuations ICMF 2009, Pisa, IT, 14-19 June, 2009
20. K. Vad: Pillantás a jövőbe: a napenergia társadalma, A Magyar Tudomány Ünnepe, Debrecen,November 5., 2009
21. Z. Labadi, A. Nemeth: Napelemtechnológiai kutatás-fejlesztés az MTA MFA-ban, ELFT és Hungarian Vacuum Society szeminárium, Budapest, December 8., 2009
22. Z. Labadi, A. Nemeth, I. Barsony: Napelemtechnológiai Innovációs Centrum az MTA MFA-ban, ELFT Anyagtudományi Őszi Iskola, Gyöngyöstarján, Szeptember 30., 2009
23. J. Toth, J. Pazman, A. Nemeth, A. Csik, Z. Labadi, L. Köver, I. Cserny, D. Varga, Z. Gacsi: XAES studies of thin ZnO(Al) layers anbd SiC particles, JVC 13 Conference, Strbske Pleso, Slovakia, 20-24 June, 2010
24. Z. Labadi, A. Nemeth, A. Buzas, Z. Geretovszky, C. Major, C. Ducso, I. Barsony: Adaptation of ZnO TCO process to thin film PV applications, 25th European PV Solar Energy Conference, Valencia, Spain, 6-10 Septembre, 2010
25. Z. Labadi, A. Nemeth, G. Molnar, M. Fried, I. Barsony: Atomic Layer Deposition and characterisation of ZnO thin films for CIGS solar cell buffer layer, E-MRS Spring Meeting, Strasbourg, France, 7-11 June, 2010
26. J. Toth, J. Pazman, A. Nemeth, A. Csik, Z. Labadi, L. Köver, I. Cserny, D. Varga, Z. Gacsi: XAES studies of thin ZnO(Al) layers and SiC particles, JVC 13 Conference, Strbske Pleso, Slovakia, 20-24 June, 2011
27. Zs. Baji, Z. Lábadi, M. Fried, Zs. Horváth, I. Bársony, Characterization of Al doped ALD ZnO layers, E-MRS Spring Meeting, Nice, France, 9-13 May, 2011
28. Z. Baji, Z. Lábadi, Z. E.. Horváth, M. Fried, B. Szentpáli and I. Bársony, Al doped ALD ZnO for CIGS buffer layer, poster, 26th European Photovoltaic Solar Energy

Conference and Exhibition (26th EU PVSEC), Hamburg, Germany, 5-9 September 2011

29. Z. Baji , Z. Lábadi , M. Fried K. Vad J. Toth and I. Bársony, Al doped ALD ZnO for CIGS buffer layer EUPVSEC Proceedings, 2011, 2992 - 2997 ISBN: 3-936338-27-2 DOI: 10.4229/26th EUPVSEC2011-3DV.2.26
30. Zs. Baji: The nucleation and growth modes of ALD ZnO, Metal Oxide / Polymer Nanocomposites and Applications (MOPNA) workshop, Budapest, 19-21 September 2011
31. Zs. Baji, Z. Labadi, Gy. Molnar, A. L. Toth, K. Vad, I. Barsony, Properties of CIGS films deposited by flash evaporation and postselenization, Poster B P3 26, presented at EMRS-2012 Spring meeting, Strasbourg, France, 14-18 May, 2012
32. Zs. Baji, J. Volk, A.L.Toth, Z. Labadi, M.Fried, I. Barsony, Ellipsometry characterization of porous Silicon coated by ALD ZnO, Oral presentation W XI 14, presented at EMRS-2012 Spring meeting, Strasbourg, France, 14-18 May, 2012
33. Zs. Baji, Z. Lábadi, M. Fried, Zs. Horváth, B. Pécz, I. Bársony, Growth and characterization of epitaxial ALD ZnO layers Poster Q P1 39, presented at EMRS-2012 Spring meeting, Strasbourg, France, 14-18 May, 2012